



**University of
Zurich^{UZH}**

**Zurich Open Repository and
Archive**

University of Zurich
University Library
Strickhofstrasse 39
CH-8057 Zurich
www.zora.uzh.ch

Year: 2015

Molecular Consequences of the SERPINH1/HSP47 Mutation in the Dachshund Natural Model of Osteogenesis Imperfecta.

Lindert, Uschi ; Weis, Mary Ann ; Rai, Jyoti ; Seeliger, Frank ; Hausser, Ingrid ; Leeb, Tosso ; Eyre,
David ; Rohrbach, Marianne ; Giunta, Cecilia

Abstract: Osteogenesis imperfecta (OI) is a heritable connective tissue disease characterized by bone fragility and increased risk of fractures. Up to now, mutations in at least 18 genes have been associated with dominant and recessive forms of OI that affect the production or post-translational processing of procollagen or alter bone homeostasis. Among those, SERPINH1 encoding heat shock protein 47 (HSP47), a chaperone exclusive for collagen folding in the ER, was identified to cause a severe form of OI in dachshunds (L326P) as well as in humans (one single case with a L78P mutation). To elucidate the disease mechanism underlying OI in the dog model, we applied a range of biochemical assays to mutant and control skin fibroblasts as well as on bone samples. These experiments revealed that type I collagen synthesized by mutant cells had decreased electrophoretic mobility. Procollagen was retained intracellularly with concomitant dilation of ER cisternae and activation of the ER stress response markers GRP78 and phospho-eIF2, thus suggesting a defect in procollagen processing. In line with the migration shift detected on SDS-PAGE of cell culture collagen, extracts of bone collagen from the OI dog showed a similar mobility shift, and on tandem mass spectrometry, the chains were post-translationally overmodified. The bone collagen had a higher content of pyridinoline than control dog bone. We conclude that the SERPINH1 mutation in this naturally occurring model of OI impairs how HSP47 acts as a chaperone in the ER. This results in abnormal post-translational modification and cross-linking of the bone collagen.

DOI: <https://doi.org/10.1074/jbc.M115.661025>

Posted at the Zurich Open Repository and Archive, University of Zurich

ZORA URL: <https://doi.org/10.5167/uzh-118672>

Journal Article

Accepted Version

Originally published at:

Lindert, Uschi; Weis, Mary Ann; Rai, Jyoti; Seeliger, Frank; Hausser, Ingrid; Leeb, Tosso; Eyre, David; Rohrbach, Marianne; Giunta, Cecilia (2015). Molecular Consequences of the SERPINH1/HSP47 Mutation in the Dachshund Natural Model of Osteogenesis Imperfecta. *Journal of Biological Chemistry*, 290(29):17679-89.

DOI: <https://doi.org/10.1074/jbc.M115.661025>

Molecular Consequences of Defective *SERPINH1*/HSP47 in the Dachshund Natural Model of Osteogenesis Imperfecta

Uschi Lindert¹, Mary Ann Weis², Jyoti Rai², Frank Seeliger³, Ingrid Hausser⁴, Tosso Leeb⁵, David Eyre², Marianne Rohrbach¹, Cecilia Giunta^{1,6}

¹Division of Metabolism, Connective Tissue Unit, University Children's Hospital Zurich, Children's Research Center, Zurich, Switzerland

²Department of Orthopaedics and Sports Medicine, University of Washington, Seattle, WA, USA

³AstraZeneca, Drug Safety and Metabolism, Mölndal, Sweden

⁴Institute of Pathology, University Hospital Heidelberg and Electron Microscopy Core Facility, Heidelberg University, Germany

⁵Institute of Genetics, Vetsuisse Faculty, University of Bern, Bern, Switzerland

Running Title: *The collagen I chaperone HSP47 in Osteogenesis Imperfecta*

⁶**To whom correspondence should be addressed:** Division of Metabolism, Connective Tissue Unit, University Children's Hospital Zurich, Steinwiesstrasse 75, 8032 Zurich, Switzerland, Tel: Tel. +41 44 266 77 58, E-mail: Cecilia.Giunta@kispi.uzh.ch

Keywords: Osteogenesis, collagen, heat shock protein 47, *SERPINH1*, connective tissue, extracellular matrix, bone, cross-links, endoplasmic reticulum stress (ER stress)

Background: The collagen chaperone HSP47 is implicated in recessive osteogenesis imperfecta (OI).

Results: In OI-Dachshunds, an HSP47(Leu326Pro) mutation affects the post-translational modification, secretion and cross-linking of collagen type I.

Conclusion: Impaired chaperone function, ER stress and aberrant bone collagen cross-linking are implicated in the disease mechanism.

Significance: Our findings are relevant for the diagnosis and pathological understanding of OI caused by an HSP47 defect.

ABSTRACT

Osteogenesis imperfecta (OI) is a heritable connective tissue disease characterized by bone fragility and increased risk of fractures. Up to now, mutations in at least eighteen genes have been associated with dominant and recessive forms of OI that affect the production or post-translational processing of procollagen or alter bone homeostasis. Among those, *SERPINH1* encoding heat shock protein 47 (HSP47), a

chaperone exclusive for collagen folding in the ER, was identified to cause a severe form of OI in Dachshunds (Leu326Pro) as well as in humans (one single case with a Leu78Pro mutation). To elucidate the disease mechanism underlying OI in the dog model, we applied a range of biochemical assays to mutant and control skin fibroblasts as well as on bone samples. These experiments revealed that type I collagen synthesized by mutant cells had decreased electrophoretic mobility. Procollagen was retained intracellularly with concomitant dilation of ER cisternae and activation of the ER stress response markers GRP78 and P-eIF2 α , thus suggesting a defect in procollagen processing. In line with the migration shift detected on SDS-PAGE of cell culture collagen, extracts of bone collagen from the OI-dog showed a similar mobility shift and on tandem mass spectrometry the chains were post-translationally overmodified. The bone collagen had a higher content of pyridinoline than control dog bone. We conclude that the *SERPINH1* mutation in this naturally

occurring model of OI impairs how HSP47 acts as a chaperone in the ER. This results in abnormal post-translational modification and cross-linking of the bone collagen.

Osteogenesis imperfecta (OI) or “brittle bone disease” is a heterogeneous heritable disorder of bone matrix formation and homeostasis. Its cardinal manifestations are low bone mass and reduced bone strength, leading to increased bone fragility and deformity. Other common clinical findings include short stature, progressive conductive hearing loss, blue-grey sclerae as well as brittle opalescent teeth (dentinogenesis imperfecta).

In approximately 90% of individuals with the clinical diagnosis of OI, dominant mutations in the type I collagen coding genes *COL1A1* (OMIM 120150) and *COL1A2* (OMIM 120160) are responsible for the disorder (1). Over the last eight years, mutations in several noncollagenous genes involved in the post-translational processing of procollagen I, in osteoblast-specific signaling or in gene regulation have been characterized in either dominant or recessive forms of OI: *CRTAP* (OMIM 605497), *LEPRE1* (OMIM 610339), *PPIB* (OMIM 123841), *PLOD2* (OMIM 601865), *FKBP10* (OMIM 607063), *BMP1* (OMIM 112264), *CREB3L1* (Entrez ID 90993), *IFITM5* (OMIM 614757), *PLS3* (OMIM 300131), *TMEM38B* (OMIM 611236), *WNT1* (OMIM 164820), *SP7* (OMIM 606633), *SERPINF1* (OMIM 172860), *SERPINH1* (OMIM 600943) (2) and most recently P4HB (OMIM 176790) (3) and SEC24D (OMIM 607186) (4).

Type I collagen, the major extracellular matrix component of bone, is a triple helical molecule composed of two pro- $\alpha 1$ (I) chains and one pro- $\alpha 2$ (I) chain, encoded by *COL1A1* and *COL1A2*, respectively. In the rough endoplasmic reticulum (rER), folding of the three pro- α chains into a triple helix begins at their C-terminal end and proceeds in a zipper-like fashion towards the N-propeptide (5). To allow for the folding of procollagen chains into the triple helix, modifying enzymes such as prolyl hydroxylases and several ER chaperones are needed (6).

Among them, HSP47 encoded by *SERPINH1* acts as a collagen-specific chaperone (7) that preferentially binds the folded triple-helix, thus stabilizing the structure (8-9). It is also

believed to prevent the lateral aggregation of procollagen triple helices in the ER (10) and guard their transport from the ER to the cis-Golgi (11-12). In the Golgi, the pH drop releases bound HSP47 which is recycled back to the ER by its C-terminal RDEL sequence (13-14).

In Dachshunds, a p.Leu326Pro mutation in HSP47 was found to cause a severe recessive form of OI characterized by marked osteopenia, thin bones with inhomogeneous and shallow trabeculation in the entire foreleg, joint hyperlaxity and undermineralization of the teeth (dentinogenesis imperfecta) (15). Previous clinical and histological investigations in OI-Dachshunds, performed before the mutation had been identified, have revealed bone fragility due to a paucity of cancellous and cortical lamellar bone (16). In humans, a single case with a severe form of OI due to a homozygous missense mutation (p.Leu78Pro) rendering the HSP47 protein instable has been reported (17). In mice, the knock-out of Hsp47 resulted in embryonic lethality around day 11 post coitum, suggesting a pivotal role during development (18).

Even though previous studies in humans and mice have demonstrated the importance of HSP47 for the formation of type I collagen, the underlying pathomechanism leading to OI is not well understood. Therefore, we set out to biochemically characterize this naturally occurring OI dog model, to further understand the role of HSP47 in procollagen processing and bone formation, and thereby to enhance our understanding of the pathology of OI.

EXPERIMENTAL PROCEDURES

Cell culture—Primary fibroblast cultures were established from skin biopsies of an affected 10-week-old Dachshund (OI) and two control dogs, a Bernese mountain dog (Contr. 1) and a 3-year-old mongrel (Contr. 2), by explant culture. Cells were grown in standard cell culture medium composed of DMEM (Gibco, 31966) supplemented with 10% fetal calf serum, 100 units/mL of penicillin, 100 μ g/mL of streptomycin and 0,25 μ g/mL of amphotericin B (Gibco).

Collagen synthesis and secretion analysis—For steady-state analysis of collagen produced in vitro by cultured fibroblasts, the cells were seeded into 6-well culture plates (250,000 cells/well). After 24 hours, the cell culture medium was replaced by serum-free MEM

(Gibco, 41090) supplemented with 50 µg/ml ascorbate, 50 µg/ml catalase, 10 µCi 2,3 (³H)-proline and 10 µCi 2 (³H)-glycine (PerkinElmer) for 16 hours. The medium and cell layers were harvested, digested with 25 µM pepsin in Hank's Balanced Salt Solution (Gibco) for 2 hours, precipitated with ethanol and analysed on a 5% polyacrylamide gel containing 0.1% SDS and 0.5 M urea. After fixation in sulphosalicylic acid / trichloroacetic acid the gel was impregnated with 2,5- diphenyloxazole (43.4 g in 200 ml DMSO) and subjected to fluorography.

For the pulse-chase analysis, fibroblasts were seeded into 3.5 cm-tissue culture plates at 250,000 cells/dish, allowed to settle overnight, and then were incubated in cell culture medium supplemented with 50 µM ascorbate for 24 hours. The cells were pulse-labeled in MEM supplemented with 50 µM ascorbate, 30 µCi 2,3 (³H)-proline and 30 µCi 2 (³H)-glycine for 20 minutes. The cells were then chased for 0, 20, 40 and 80 minutes in MEM supplemented with 2 mM unlabeled proline and 2 mM unlabeled glycine. At the end of each chase, the medium and cell layers were harvested separately, digested with pepsin and subjected to fluorography. The quantification was done using the Gel Logic 6000Pro Imager (Carestream) and the Carestream Molecular Imaging Software. The experiment was performed twice with similar results.

Western blot analysis of HSP47, P-eIF2α and GRP78—Fibroblasts were seeded into T75 flasks and grown to confluency. Whole cell extracts were prepared by lysing cells in NP-40-buffer (50 mM Tris/HCl, pH 8, 125 mM NaCl, 1% NP-40, 1 mM EDTA, 1 mM PMSF) and protease inhibitor cocktail (Roche) for 45 minutes on ice. For the induction of ER stress or proteasome inhibition, cells were treated with 0.5 µM thapsigargin (Sigma) for 4 hours or 50 µM MG-132 (Enzo Life Sciences) for 16 hours, respectively, prior to harvesting. 50 µg of protein were analyzed on a 10% SDS-gel, followed by western blot. The following antibodies were used: mouse anti-HSP47 (ADI-SPA-470-D; ENZO Life Sciences) at 1:1000; rabbit anti-GRP78 (Abcam) at 1:1000; Phospho-eIF2α-(Ser51) (#9721; CST) at 1:1000; mouse anti-actin (A1978; Sigma) at 1:3000; goat anti-mouse HRP (sc-2302; Santa Cruz) at 1:3000 and goat anti-rabbit HRP (sc-2301; Santa Cruz) at 1:3000. The blots were developed using the ECL-system (GE Healthcare

Lifesciences), and quantified using the Gel Logic 6000Pro (Carestream) and the Carestream Molecular Imaging Software. For the calculation of standard deviations, three independent experiments were combined.

Immunofluorescent staining—Fibroblasts were split from a confluent T75 flask and seeded onto glass cover slips in 12-well tissue culture plates. After 24 hours the cells were fixed either in ice-cold methanol for five minutes (for anti-HSP47) or in 4% PFA for 10 minutes followed by incubation in ice-cold methanol for one minute (for anti-Col I). Cells were washed three times in PBS (10 mM Na₂HPO₄, 2 mM KH₂PO₄, 137 mM NaCl, 2.7 mM KCl) and incubated in blocking buffer (1% BSA, 10% FCS, 0.3 M glycine, 0.1% Tween-20 in PBS) for one hour at room temperature. The cells were then incubated with the respective primary antibodies diluted in blocking buffer for 1.5 hours at room temperature, washed three times in PBS, and incubated with the secondary antibodies diluted in blocking buffer for one hour at room temperature. After washing three times in PBS the cover slips were mounted onto glass slides using SlowFade Gold antifade mountant (S36939, Molecular Probes) containing 4'-6-diamidino-2-phenylindole (DAPI) for nuclear staining. Images were taken on a fluorescence microscope (Leica HC DMIL equipped with a Leica DFC420 digital camera).

Primary antibodies: mouse anti-HSP47 (M16.10A1, ADI-SPA-470) from Enzo Life Sciences (1:100); rabbit anti-GRP78 (ab32618) from Abcam (1:100); mouse anti-Collagen I (ab6308) from Abcam (1:100); rabbit anti-GM130 (ab52649) from Abcam (1:100). Secondary antibodies: goat anti-rabbit Alexa Fluor 568 (ab175471) from Abcam (1:500) and goat anti-mouse Alexa Fluor 488 (A11017) from Molecular Probes (1:500).

Electron microscopy of cultured primary fibroblasts—Fibroblasts were seeded into T75 flasks and grown to confluency (two flasks per sample). Then, the cells were washed twice in 8 ml ice-cold Hank's Balanced Salt Solution (Gibco) and fixed in 3 ml fixation solution (3% glutaraldehyde (Sigma) in 0.1 M cacodylate buffer pH 7.4) for 16 hours at 4°C. The fixation solution was removed and the cells were harvested using a rubber policeman in 1 ml 0.1 M cacodylate buffer into 2 ml Eppendorf tubes and centrifuged at 13000 U/min for one minute. The supernatant was

discarded and the cell pellet was washed three times in 0.1 M cacodylate buffer, postfixed for one hour in 1% osmium tetroxide, dehydrated by graded series of ethanol and embedded in glycidether 100 (Roth) (formerly Epon 812). Semithin and 70-80 nm ultrathin sections were cut with a Reichert Ultracut E ultramicrotome, counterstained with uranyl acetate and lead citrate and examined with a Zeiss EM900, equipped with a CCD camera (TRS).

Tissue preparation for collagen analysis—Stored frozen tissues from an affected Dachshund pup (10 weeks) and two control dogs (9 yr large breed and 14 yr small breed) were used for analysis. Mid-shaft cortical bone and skin were scraped clean and defatted with chloroform/methanol (3:1 v/v); bone was demineralized in 0.1 M HCl, carrying out all steps at 4°C. Collagen was solubilized from each tissue by heat denaturation in SDS-PAGE sample buffer at 90°C without DTT. Demineralized bone was also extracted with pepsin in 3% acetic acid at 4°C then precipitated by adding NaCl to 0.8M.

SDS-PAGE of bone and skin collagen extracts—The method of Laemmli (19) was used with 6% gels for extracts of tissue collagen.

Cross-link analysis—Bone was hydrolyzed in 6 N HCl, dried, dissolved in 1% (v/v) n-heptafluorobutyric acid and analyzed by C18 reverse-phase HPLC as described (20).

Mass spectrometry of collagenase digested bone—Demineralized bone was digested with bacterial collagenase as described (21) and collagenase generated peptides were separated by reversed-phase HPLC (C8, Brownlee Aquapore RP-300, 4.6 mm x 25 cm) with a linear gradient of acetonitrile:n-propanol (3:1 v/v) in aqueous 0.1% (v/v) trifluoroacetic acid (22). Electrospray MS was performed on individual fractions using an LTQ XL ion-trap mass spectrometer (Thermo Scientific) equipped with in-line liquid chromatography using a C4 5 µm capillary column (300 µm x 150 mm; Higgins Analytical RS-15M3-W045) eluted at 4.5 µl/min. The LC mobile phase consisted of buffer A (0.1% formic acid in MilliQ water) and buffer B (0.1% formic acid in 3:1 acetonitrile:n-propanol v/v). The LC sample stream was introduced into the mass spectrometer by electrospray ionization (ESI) with a spray voltage of 4 kV. Proteome Discoverer search software (Thermo Scientific) was used for peptide identification using the NCBI protein database.

Proline and lysine modifications were examined manually by scrolling or averaging the full scan over several minutes so that all of the post-translational variations of a given peptide appeared together in the full scan.

RESULTS

Protein stability and normal localization of HSP47(p.Leu326Pro) in dog primary fibroblasts—To test whether the Leu326Pro mutation has any effect on the expression and stability of the HSP47 protein, we performed western blot analysis and immunofluorescent staining in cultured fibroblasts. In the western blot analysis, the amount of HSP47 in the mutant fibroblasts was reduced by half compared to the control (Fig. 1a and 1b). Upon proteasome inhibition using MG-132 the amount of protein was not increased further. The immunofluorescent staining of HSP47 showed that the protein was similarly detectable in control as well as in HSP47-mutant fibroblasts (Fig. 1c). The staining pattern was similar in mutant and control cells and co-localized with the ER marker GRP78.

HSP47 is required for efficient folding and secretion of type I procollagen—We next aimed to investigate whether the mutation in HSP47 impairs its ability to act as a chaperone thereby affecting type I procollagen folding. To this end, biochemical analyses of procollagen I were performed. The steady-state analysis of pepsinized procollagen separated by SDS-PAGE showed that in both the medium and the cell layers the bands of the collagen I α -chains had decreased electrophoretic mobility in mutant compared to control fibroblasts, and also had a broader appearance in the cell layer (Fig. 2a). Furthermore, an increased amount of procollagen I, III and V compared to the control was detected in the cell layer (Fig. 2a). Similarly, SDS-PAGE of unpepsinized procollagen showed an increased amount of the pro- α 1(I) and pro- α 2(I) chains in the cell layer and decreased electrophoretic mobility of fully processed α 1(I) and α 2(I) chains in the medium layer (Fig. 2b). Additionally, in the medium layer, the amount of fully processed α 1(I)- and α 2(I)-chains was decreased in mutant dog fibroblasts compared to control fibroblasts (Fig. 2b). These findings suggest that procollagen I is overmodified in the helical part and possibly in the telopeptide region and is less efficiently processed in the extracellular space. The increased

amounts of collagen I, III and V in the cell layer might indicate intracellular retention or decreased secretion of fibrillar collagens in HSP47-mutant cells.

We further investigated the secretion of collagen from mutant dog fibroblasts by pulse-chase analysis. In mutant fibroblasts, the secretion of type I and type V collagen from the medium into the cell layer was slightly decreased compared to the control fibroblasts (Fig. 3a and 3b). This was most evident in the 20-minute chase for type I collagen, and in the 80-minute chase for type V collagen.

Finally, co-immunofluorescent staining was performed using antibodies against the helical part of type I collagen, the ER-chaperone GRP78 and the Golgi marker GM130 (Fig. 4a and b). In agreement with the findings above, mutant cells showed a strong staining for Col I and only faint staining in two different control cell lines (Contr. 1 and Contr. 2). Furthermore, the staining pattern in control cells overlapped with the Golgi marker (Fig. 4b), but was more spread out in the OI-cells overlapping with both, the Golgi and ER marker.

Taken together, these observations point towards delayed folding and intracellular retention of procollagen I and raise the question of a possible induction of an ER stress response.

Dilation of ER cisternae and activation of the ER stress response in HSP47-mutant fibroblasts—To investigate whether the intracellular retention of collagen might cause ultrastructural alterations, transmission electron microscopy (TEM) was performed on cultured fibroblasts from the HSP47-mutant and a control dog. Dilation of the endoplasmic reticulum in the mutant fibroblasts was more pronounced than in the control cells (Fig. 5). To test for the activation of an ER stress response, GRP78 and Phospho-eIF2 α which are induced upon accumulation of unfolded proteins, were analysed by western blot (Fig. 6a – 6d). In HSP47-mutant cells, the amount of GRP78 (Fig. 6a and 6b) as well as Phospho-eIF2 α (Fig. 6c and 6d) was increased compared to control cells. Exposure to the ER stress inducer thapsigargin (Thap) lead to an increase in control cells, whereas it remained at the high level in the HSP47-mutant cells. Induction of autophagy was not observed in western blot analysis testing for LC3B lipidation (data not shown).

Overhydroxylation and altered cross-linking of bone collagen—To investigate whether the

overmodification of collagen observed in cultured skin fibroblasts was evident in HSP47-mutant dog tissue we directly analysed collagens extracted from bone and skin (Fig. 7). Chain mobilities were clearly slower from mutant compared with control dog tissues. Individual collagen chains were excised from the SDS-PAGE gel, subjected to trypsin digestion and lysine hydroxylation was assessed by tandem mass spectrometry (TMS) in targeted peptides from bone collagen of an HSP47-mutant dog and two control dogs. The TMS analysis revealed an increase in helix and telopeptide lysine modification (Fig. 8). Residue K87 was overglycosylated as glucosyl-galactosyl-hydroxylysine (glcgalHyl) in the mutant compared with galactosyl-hydroxylysine (gal Hyl) in the controls and K930 was essentially all Hyl in the mutant but mostly Lys in control bone. From the same trypsin digests 3-hydroxylation of Pro986 was found to be essentially complete and indistinguishable from that in controls.

Further analysis of pyridinoline cross-links in total hydrolysates of bone collagen showed an increase in the total pyridinoline content (HP+LP moles per mole of collagen) and in the ratio of hydroxylysyl pyridinoline (HP) to lysyl pyridinoline (LP) in the mutant bone compared with bone of two control dogs (Table 1). Furthermore, pyrrole cross-links were not detectable on reaction of decalcified mutant bone with Ehrlich's reagent but strongly reactive in control dog and human bone (data not shown).

DISCUSSION

SERPINH1, encoding HSP47, is a chaperone essential for efficient folding of collagen triple-helices in the ER, thereby possibly preventing their aggregation in the ER, and facilitating their transport into the Golgi (7,9-12). Its pivotal role in bone formation became evident when it was shown to cause a recessive form of osteogenesis imperfecta (OI) in the Dachshund (15) and then in humans (17). However, the disease mechanism is not well understood. Here, we provide a detailed biochemical analysis, showing that the HSP47-mutation in the dog is characterized by overmodification and intracellular retention of procollagen type I, dilation of ER cisternae and upregulation of the ER stress markers GRP78 and P-eIF2 α *in vitro* as well as by aberrant bone collagen cross-linking *in vivo*. Furthermore, we compare our findings with those recently made in

the human OI-case (17) and in HSP47 knock-out mice (18,23) (summarized in Table 2), and discuss their implications for procollagen I processing and bone formation in the context of understanding the pathomechanism of OI.

In the reported human OI-case, the mutant HSP47 was unstable and only detectable upon proteasome inhibition (17), providing an explanation for its loss of function. In our study, we show that the mutant HSP47 in the dog was clearly detectable by immunofluorescent staining and by western blot, although the latter analysis showed a decrease by half (Fig. 1). However, it seems unlikely that this decrease in the amount of HSP47 causes the OI-pathology, since mice heterozygous for the knock-out were phenotypically normal and procollagen I processing and protease-sensitivity were similar to wild type despite a marked decrease in HSP47 (18). More likely, the HSP47 mutation in the dog leads to structural alterations and some loss of function. For example, aggregation or polymerization of mutant HSP47 in the ER – as has been observed for mutations in other members of the serpin family in so-called serpinopathies (24) – could affect its availability as a chaperone, and provide an explanation for its stability.

It is presumed that mutations in genes coding for collagen chains or their chaperones can delay procollagen triple helix formation, leading to prolonged exposure of the nascent chains to hydroxyl- and glycosyl-transferases in the ER. Thus, slower migration of the $\alpha 1(I)$, $\alpha 2(I)$ and β -chains of collagen type I is often detected by SDS-PAGE analysis in cultured fibroblasts from OI-patients with mutations in *COL1A1*, *COL1A2*, *CRTAP*, *LEPRE1* or *PPIB* (25-28). In the human HSP47-OI case, migration of cell culture collagen was reported to be normal. In the OI-dog, we observed slower migration of type I collagen chains from cell lysates, from culture medium and from bone matrix extracts (Fig. 2 and Fig. 7). This points towards at least a partial loss of the HSP47 chaperone function leading to delayed folding or to local micro-unfolding of the collagen triple helix, thus allowing for increased posttranslational modification of collagen (see proposed mechanism, Figure 9). The findings further indicate that incorrectly modified collagen is secreted into the extracellular space *in vitro*, which may contribute to the OI-pathology. The reason for the different findings between the human and

the dog cases remains unclear. They may have been due to the different mutations (p.Leu326Pro vs p.Leu78Pro). Alternatively, post-translational overmodification in the human case may have been less obvious in cell culture and since no bone was available for analysis any effect on collagen cross-linking is unknown (17).

The observation of overmodified collagen *in vitro* was supported by tandem mass spectrometry (TMS) of bone collagen from an affected dog showing markedly increased modification levels of lysine at cross-linking sites in the helix and both telopeptides. Other non-cross-linking lysines in the helix also showed increased hydroxylation (Fig. 8 and data not shown). Direct analysis of mature cross-links, showed more than double the content of total pyridinolines (HP+LP) as well as an increased HP/LP ratio (Table 1) consistent with the TMS results on their linear precursor sequences (Fig. 8). In normal bone collagen, the predominant mature cross-links are pyrroles and pyridinolines, which are usually present in equal molar amounts (21,29). In essence two telopeptide lysine residues and one helix lysine contribute to each cross-link, so the extent of hydroxylation of these lysines determines the cross-link chemistry. Two telopeptide hydroxylysines produce pyridinolines, whereas pyrrole cross-links form when one of the two telopeptide lysines is unhydroxylated (30). Thus, the shift from pyrrole to pyridinoline cross-links evident in mutant dog bone is consistent with the apparent complete telopeptide lysine hydroxylation (Fig. 8). Similarly, the increase in helix lysine hydroxylation in bone of the HSP47-mutant dog is responsible for the increased HP/LP ratio.

One limitation of the tissue studies, however, was the lack of age-matched normal dog tissues for direct comparison. It is possible therefore that some of the modification increase is age-related.

It is notable that variations in relative contents of pyrrole and pyridinoline cross-links have been associated with differences in human vertebral trabecular bone morphologies (31). In bone of OI-Dachshunds, the development of secondary spongiosa was noted to be defective (16). This suggests that the overhydroxylated type I collagen in the extracellular matrix might disturb the bone-specific cross-linking of type I collagen and negatively influence trabecular bone formation, thereby contributing to the OI-pathology. Abnormal collagen cross-linking is

characteristic of several subtypes of OI including Bruck syndrome, in which bone collagen lacks pyridinolines, and subtypes of the Ehlers-Danlos syndrome, in both of which the diagnosis can be confirmed by analysis of pyridinoline cross-links in urine (28,30,32-35).

The accumulation or retention of collagen in HSP47-mutant cells was consistently observed from mouse (23), human (17) and, in the present study, dog using pulse-chase (Fig. 3) and immunofluorescent staining methods (Fig. 4) as well as steady-state analysis of collagen and procollagen type I (Fig. 2). There is some discrepancy in the site of observed intracellular collagen accumulation. In the human case, Christiansen et al. showed that type I procollagen was diminished in the ER and accumulated in the Golgi (17), while in the mouse HSP47 knock-out cells procollagen I accumulated in the ER (23). Interestingly, immunofluorescent staining in dog fibroblasts also displayed increased staining of procollagen I in the ER. Although this could reflect distinct pathomechanisms leading to OI in the human and dog cases, an alternative explanation is the use of different antibodies. In the mouse and in the present study an antibody directed against the triple helix of collagen was used, whereas in the human case the antibody detected the N-propeptide of the pro- α 1(I) chain. Retention of procollagen type I in the ER in the OI-dog is supported by the present findings of an activated ER stress response (Fig. 6) and enlarged

ER cisternae seen on transmission electron microscopy (TEM) (Fig. 5) in cultured fibroblasts. Indeed, similar observations have been made by TEM in fibroblasts from HSP47 knock-out mice (23) and in osteoblasts in bone from an OI-Dachshund (16). Thus, our findings suggest that activation of the ER stress response by misfolded and retained procollagen could play a role in the pathomechanism of OI in the Dachshund. Mutant HSP47 aggregating or polymerizing in the ER as discussed above, might further contribute to ER stress. Involvement of ER stress has already been discussed as being implicated in OI and increased apoptosis, impaired differentiation and decreased activity or survival of osteoblasts have been proposed as possible pathomechanisms (36-39).

Taken together, our findings suggest an impairment of the HSP47 chaperone function in the ER, leading to overhydroxylation and partial intracellular retention of procollagen I. Both consequences – ER stress and aberrant bone collagen cross-linking – have the potential to play a causative role in the OI-pathology and further studies are required to determine their individual significance. Finally, with regard to diagnostics of OI caused by a mutation in HSP47, overmodification of collagen I may be evident in fibroblast cultures on SDS-PAGE analysis, and an increased HP/LP ratio of bone collagen is potentially detectable by urinary pyridinoline analysis.

ACKNOWLEDGEMENTS

We thank Angelika Schwarze and Danuta Waschke for expert technical assistance with fibroblast cultures. The work was supported by the SNF (grant Nr. 310030_138288) and the Gottfried und Julia Bangerter-Rhyner-Stiftung.

CONFLICT OF INTEREST

The authors declare that they have no conflicts of interest with the contents of this article.

AUTHOR CONTRIBUTION

CG, MR and UL designed the study and wrote the paper. UL designed, performed and analyzed the experiments shown in Figures 1, 2, 3, 4 and 6. UL and CG designed Figure 9. MAW, JR and DE, performed and analyzed the experiments shown in Figures 7 and 8 and in Table 1 and DE critically revised the manuscript. IH performed the transmission electron microscopy shown in Figure 5 and critically revised the manuscript. TL and FS provided dog tissue samples, established dermal fibroblast cultures and critically revised the manuscript. All authors reviewed the results and approved the final version of the manuscript.

REFERENCES

1. Rohrbach, M., and Giunta, C. (2012) Recessive osteogenesis imperfecta: clinical, radiological, and molecular findings. *Am. J. Med. Genet. C Semin. Med. Genet.* **160C**, 175-189
2. Van Dijk, F. S., and Sillence, D. O. (2014) Osteogenesis imperfecta: clinical diagnosis, nomenclature and severity assessment. *Am. J. Med. Genet. A* **164A**, 1470-1481
3. Rauch, F., Fahiminiya, S., Majewski, J., Carrot-Zhang, J., Boudko, S., Glorieux, F., Mort, J. S., Bachinger, H. P., and Moffatt, P. (2015) Cole-Carpenter syndrome is caused by a heterozygous missense mutation in P4HB. *Am J Hum Genet* **96**, 425-431
4. Garbes, L., Kim, K., Riess, A., Hoyer-Kuhn, H., Beleggia, F., Bevon, A., Kim, M. J., Huh, Y. H., Kweon, H. S., Savarirayan, R., Amor, D., Kakadia, P. M., Lindig, T., Kagan, K. O., Becker, J., Boyadjev, S. A., Wollnik, B., Semler, O., Bohlander, S. K., Kim, J., and Netzer, C. (2015) Mutations in SEC24D, encoding a component of the COPII machinery, cause a syndromic form of osteogenesis imperfecta. *Am J Hum Genet* **96**, 432-439
5. Engel, J., and Prockop, D. J. (1991) The zipper-like folding of collagen triple helices and the effects of mutations that disrupt the zipper. *Annu. Rev. Biophys. Biophys. Chem.* **20**, 137-152
6. Lamande, S. R., and Bateman, J. F. (1999) Procollagen folding and assembly: the role of endoplasmic reticulum enzymes and molecular chaperones. *Semin. Cell Dev. Biol.* **10**, 455-464
7. Nagata, K. (1996) Hsp47: a collagen-specific molecular chaperone. *Trends Biochem. Sci.* **21**, 22-26
8. Makareeva, E., and Leikin, S. (2007) Procollagen triple helix assembly: an unconventional chaperone-assisted folding paradigm. *PLoS One* **2**, e1029
9. Widmer, C., Gebauer, J. M., Brunstein, E., Rosenbaum, S., Zaucke, F., Drogemuller, C., Leeb, T., and Baumann, U. (2012) Molecular basis for the action of the collagen-specific chaperone Hsp47/SERPINH1 and its structure-specific client recognition. *Proc. Nat. Acad. Sci. U. S. A.* **109**, 13243-13247
10. Thomson, C. A., and Ananthanarayanan, V. S. (2000) Structure-function studies on hsp47: pH-dependent inhibition of collagen fibril formation in vitro. *Biochem. J.* **349 Pt 3**, 877-883
11. Nagata, K. (1998) Expression and function of heat shock protein 47: a collagen-specific molecular chaperone in the endoplasmic reticulum. *Matrix Biol.* **16**, 379-386
12. Smith, T., Ferreira, L. R., Hebert, C., Norris, K., and Sauk, J. J. (1995) Hsp47 and cyclophilin B traverse the endoplasmic reticulum with procollagen into pre-Golgi intermediate vesicles. A role for Hsp47 and cyclophilin B in the export of procollagen from the endoplasmic reticulum. *J. Biol. Chem.* **270**, 18323-18328
13. Nakai, A., Satoh, M., Hirayoshi, K., and Nagata, K. (1992) Involvement of the stress protein HSP47 in procollagen processing in the endoplasmic reticulum. *J. Cell Biol.* **117**, 903-914
14. Satoh, T., Yamada, M., Iwasaki, T., and Mori, M. (1996) Negative regulation of the gene for the preprothyrotropin-releasing hormone from the mouse by thyroid hormone requires additional factors in conjunction with thyroid hormone receptors. *J. Biol. Chem.* **271**, 27919-27926
15. Drogemuller, C., Becker, D., Brunner, A., Haase, B., Kircher, P., Seeliger, F., Fehr, M., Baumann, U., Lindblad-Toh, K., and Leeb, T. (2009) A missense mutation in the SERPINH1 gene in Dachshunds with osteogenesis imperfecta. *PLoS Genet.* **5**, e1000579
16. Seeliger, F., Leeb, T., Peters, M., Bruggmann, M., Fehr, M., and Hewicker-Trautwein, M. (2003) Osteogenesis imperfecta in two litters of dachshunds. *Vet. Pathol.* **40**, 530-539
17. Christiansen, H. E., Schwarze, U., Pyott, S. M., AlSwaid, A., Al Balwi, M., Alrasheed, S., Pepin, M. G., Weis, M. A., Eyre, D. R., and Byers, P. H. (2010) Homozygosity for a missense mutation in SERPINH1, which encodes the collagen chaperone protein HSP47, results in severe recessive osteogenesis imperfecta. *Am. J. Hum. Genet.* **86**, 389-398
18. Nagai, N., Hosokawa, M., Itoharu, S., Adachi, E., Matsushita, T., Hosokawa, N., and Nagata, K. (2000) Embryonic lethality of molecular chaperone hsp47 knockout mice is associated with defects in collagen biosynthesis. *J. Cell Biol.* **150**, 1499-1506
19. Laemmli, U. K. (1970) Cleavage of structural proteins during the assembly of the head of bacteriophage T4. *Nature* **227**, 680-685
20. Eyre, D. (1987) Collagen cross-linking amino acids. *Methods Enzymol.* **144**, 115-139
21. Hanson, D. A., and Eyre, D. R. (1996) Molecular site specificity of pyridoline and pyrrole cross-links in type I collagen of human bone. *J. Biol. Chem.* **271**, 26508-26516

22. Wu, J. J., Woods, P. E., and Eyre, D. R. (1992) Identification of cross-linking sites in bovine cartilage type IX collagen reveals an antiparallel type II-type IX molecular relationship and type IX to type IX bonding. *J. Biol. Chem.* **267**, 23007-23014
23. Ishida, Y., Kubota, H., Yamamoto, A., Kitamura, A., Bachinger, H. P., and Nagata, K. (2006) Type I collagen in Hsp47-null cells is aggregated in endoplasmic reticulum and deficient in N-propeptide processing and fibrillogenesis. *Mol. Biol. Cell* **17**, 2346-2355
24. Law, R. H., Zhang, Q., McGowan, S., Buckle, A. M., Silverman, G. A., Wong, W., Rosado, C. J., Langendorf, C. G., Pike, R. N., Bird, P. I., and Whisstock, J. C. (2006) An overview of the serpin superfamily. *Genome Biol.* **7**, 216
25. Barnes, A. M., Chang, W., Morello, R., Cabral, W. A., Weis, M., Eyre, D. R., Leikin, S., Makareeva, E., Kuznetsova, N., Uveges, T. E., Ashok, A., Flor, A. W., Mulvihill, J. J., Wilson, P. L., Sundaram, U. T., Lee, B., and Marini, J. C. (2006) Deficiency of cartilage-associated protein in recessive lethal osteogenesis imperfecta. *New Engl. J. Med.* **355**, 2757-2764
26. Cabral, W. A., Barnes, A. M., Adeyemo, A., Cushing, K., Chitayat, D., Porter, F. D., Panny, S. R., Gulamali-Majid, F., Tishkoff, S. A., Rebbeck, T. R., Gueye, S. M., Bailey-Wilson, J. E., Brody, L. C., Rotimi, C. N., and Marini, J. C. (2007) A founder mutation in LEPRE1 carried by 1.5% of West Africans and 0.4% of African Americans causes lethal recessive osteogenesis imperfecta. *Genet. Med.* **14**, 543-551
27. Cabral, W. A., Milgrom, S., Letocha, A. D., Moriarty, E., and Marini, J. C. (2006) Biochemical screening of type I collagen in osteogenesis imperfecta: detection of glycine substitutions in the amino end of the alpha chains requires supplementation by molecular analysis. *J. Med. Genet.* **43**, 685-690
28. Cabral, W. A., Perdivara, I., Weis, M., Terajima, M., Blissett, A. R., Chang, W., Perosky, J. E., Makareeva, E. N., Mertz, E. L., Leikin, S., Tomer, K. B., Kozloff, K. M., Eyre, D. R., Yamauchi, M., and Marini, J. C. (2014) Abnormal type I collagen post-translational modification and crosslinking in a cyclophilin B KO mouse model of recessive osteogenesis imperfecta. *PLoS Genet.* **10**, e1004465
29. Risteli J, E. H., Risteli L, Mansell JP, Bailey AJ (1994) Pyrrolic cross-links are as abundant in human bone type I collagen as pyridinolines. *J. Bone Miner. Res.* **9(suppl.)**, S186
30. Eyre, D. R., and Weis, M. A. (2013) Bone collagen: new clues to its mineralization mechanism from recessive osteogenesis imperfecta. *Calcif. Tissue Int.* **93**, 338-347
31. Banse, X., Devogelaer, J. P., Delloye, C., Lafosse, A., Holmyard, D., and Gryn timer, M. (2003) Irreversible perforations in vertebral trabeculae? *J. Bone Miner. Res.* **18**, 1247-1253
32. Giunta, C., Elcioglu, N. H., Albrecht, B., Eich, G., Chambaz, C., Janecke, A. R., Yeowell, H., Weis, M., Eyre, D. R., Kraenzlin, M., and Steinmann, B. (2008) Spondylocheiro dysplastic form of the Ehlers-Danlos syndrome--an autosomal-recessive entity caused by mutations in the zinc transporter gene SLC39A13. *Am. J. Hum. Genet.* **82**, 1290-1305
33. Kraenzlin, M. E., Kraenzlin, C. A., Meier, C., Giunta, C., and Steinmann, B. (2008) Automated HPLC assay for urinary collagen cross-links: effect of age, menopause, and metabolic bone diseases. *Clin. Chem.* **54**, 1546-1553
34. Schwarze, U., Cundy, T., Pyott, S. M., Christiansen, H. E., Hegde, M. R., Bank, R. A., Pals, G., Ankala, A., Conneely, K., Seaver, L., Yandow, S. M., Raney, E., Babovic-Vuksanovic, D., Stoler, J., Ben-Neriah, Z., Segel, R., Lieberman, S., Siderius, L., Al-Aqeel, A., Hannibal, M., Hudgins, L., McPherson, E., Clemens, M., Sussman, M. D., Steiner, R. D., Mahan, J., Smith, R., Anyane-Yeboah, K., Wynn, J., Chong, K., Uster, T., Aftimos, S., Sutton, V. R., Davis, E. C., Kim, L. S., Weis, M. A., Eyre, D., and Byers, P. H. (2013) Mutations in FKBP10, which result in Bruck syndrome and recessive forms of osteogenesis imperfecta, inhibit the hydroxylation of telopeptide lysines in bone collagen. *Hum. Mol. Genet.* **22**, 1-17
35. Steinmann, B., Eyre, D. R., and Shao, P. (1995) Urinary pyridinoline cross-links in Ehlers-Danlos syndrome type VI. *Am. J. Hum. Genet.* **57**, 1505-1508
36. Chessler, S. D., and Byers, P. H. (1993) BiP binds type I procollagen pro alpha chains with mutations in the carboxyl-terminal propeptide synthesized by cells from patients with osteogenesis imperfecta. *J. Biol. Chem.* **268**, 18226-18233
37. Forlino, A., Tani, C., Rossi, A., Lupi, A., Campari, E., Gualeni, B., Bianchi, L., Armini, A., Cetta, G., Bini, L., and Marini, J. C. (2007) Differential expression of both extracellular and intracellular proteins is involved in the lethal or nonlethal phenotypic variation of BrtlIV, a murine model for osteogenesis imperfecta. *Proteomics* **7**, 1877-1891

38. Lisse, T. S., Thiele, F., Fuchs, H., Hans, W., Przemeck, G. K., Abe, K., Rathkolb, B., Quintanilla-Martinez, L., Hoelzlwimmer, G., Helfrich, M., Wolf, E., Ralston, S. H., and Hrade de Angelis, M. (2008) ER stress-mediated apoptosis in a new mouse model of osteogenesis imperfecta. *PLoS Genet.* **4**, e7
39. Makareeva, E., Aviles, N. A., and Leikin, S. (2011) Chaperoning osteogenesis: new protein-folding disease paradigms. *Trends Cell Biol.* **21**, 168-176

FOOTNOTES

⁶To whom correspondence should be addressed: Cecilia Giunta, Division of Metabolism, Connective Tissue Unit, University Children's Hospital Zurich, Steinwiesstrasse 75, 8032 Zurich, Switzerland, Tel: Tel. +41 44 266 77 58, E-mail: Cecilia.Giunta@kispi.uzh.ch

⁸The abbreviations used are: OI, osteogenesis imperfecta; HSP47, heat shock protein 47; ER, endoplasmic reticulum; GRP78, glucose-regulated protein 78; TMS, tandem mass spectrometry; GM130, golgin A2; TEM, transmission electron microscopy; Thap, thapsigargin; HP, hydroxylysyl pyridinoline; LP, lysyl pyridinoline; Hyl, hydroxylysine; glc, glucosyl; gal, galactosyl.

FIGURE LEGENDS

FIGURE 1. Mutant HSP47 is expressed as a stable protein and localizes to the ER. (A,B) Western blot of HSP47 in primary cultured fibroblasts of mutant (OI) and a control dog (Contr. 1). The mutant protein level is reduced to half of the control level. Proteasome inhibition by treatment with MG-132 (50 μ M, 16 h) does not influence the amount of either mutant or wild-type protein. **(B)** Immunofluorescent staining of HSP47 in primary cultured fibroblasts of mutant and control dog. The protein is similarly detectable in both mutant and control fibroblasts and co-localizes with the endoplasmic reticulum marker GRP78. Cell nuclei stained with DAPI are shown in blue.

FIGURE 2. Overmodification of type I collagen and intracellular retention of type I, III and V collagen in HSP47-mutant fibroblasts. Steady-state analysis of **(A)** pepsinized and **(B)** unpepsinized procollagen by SDS-PAGE in primary cultured fibroblasts of HSP47-mutant (OI) and control dog (Contr. 1). The pro α 1(I) and pro α 2(I) (in 2B) as well as the α 1(I) and α 2(I) (in 2A) bands from mutant fibroblasts show decreased electrophoretic mobility compared to the control, indicating overmodification of the triple-helical and possibly the telopeptide region. Pro α 1(I) and pro α 2(I) are retained in the cell layer. Also, type III and type V collagen are retained in the cell layer as evident in the pepsinized collagen analysis **(2A)**.

FIGURE 3. Delayed secretion of type I and type V collagen. (A) Pulse-chase analysis of pepsinized collagen in primary fibroblasts showing a delay in secretion of type I and type V collagen from the cell layer (C) into the medium (M) in the OI-dog (OI) when compared to the control (Contr. 1). **(B)** Quantification of the pulse-chase experiment for type I collagen.

FIGURE 4. Type I collagen accumulates in HSP47-mutant fibroblasts. Co-immunofluorescent staining of primary skin fibroblasts for type I collagen (Col I, green) and **(A)** the ER marker GRP78 or **(B)** the Golgi marker GM130, both shown in red. The two control cell lines (Contr. 1 and 2) show weak collagen I staining overlapping with the Golgi marker. In HSP47-mutant fibroblasts (OI), collagen I staining is much stronger and more spread out overlapping with both, the ER marker and the Golgi marker.

FIGURE 5. Dilation of endoplasmic reticulum cisternae in HSP47-mutant fibroblasts. Transmission electron microscopy of primary fibroblasts from HSP47-mutant dog (OI) showing increased abundance of enlarged endoplasmic reticulum cisternae (red arrows) compared to control dog fibroblasts (Contr. 1).

FIGURE 6. ER-stress markers are upregulated in HSP47-mutant fibroblasts. (A, C) Western blot analysis and **(B, D)** quantification of three independent experiments of GRP78 and P-eIF2 α . The amount of both ER stress marker proteins is increased in untreated (nt) HSP47-mutant fibroblasts (OI) compared

to the level in control cells (Contr. 2). Induction of ER stress by treating cells with thapsigargin (Thap.) leads to an increase in control cells, while remaining on a high level in HSP47-mutant cells. GRP78 is detected as a double band, probably due to post-translational modification.

FIGURE 7. Decreased electrophoretic mobility of type I collagen chains from HSP47-mutant bone and skin.

SDS-PAGE (6%) of type I collagen extracted by heat denaturation or pepsin from HSP47-mutant (OI) bone and heat denaturation of skin shows decreased electrophoretic mobility of the α - and β -chains compared to the 9 yr control dog (Control).

FIGURE 8. Overmodification of lysine residues at cross-linking sites in HSP47-mutant bone collagen revealed by tandem mass spectrometry.

Peptides from the four molecular sites of cross-linking in collagen type I (A) prepared by bacterial collagenase digestion of decalcified bone were identified by LCMS. Their post-translational profiles are compared between HSP47-mutant and control (9 yr) bone. Spectra from the two helical sites (K87 and K930) (B) and two telopeptide sites (C) show that K87 is mostly glcgalHyl, K930 is mostly Hyl and both telopeptides are essentially all Hyl from mutant bone, whereas from control bone K87 is mostly galHyl, K930 is highly underhydroxylated and both telopeptides are about 50% hydroxylated.

FIGURE 9. Proposed pathomechanism of OI induced by the HSP47 mutation in the dog.

HSP47 , hydroxy-lysyl residues  glucosyl-galactosyl residues 

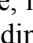
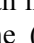
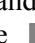
Decreased binding of HSP47 to the collagen triple helix delay collagen folding overall, and allow for local micro-unfolding of the triple helix after its formation, thus leading to an increased exposure to lysyl-hydroxylases and glucosyl-galactosyl- transferases and to increased posttranslational modification of the triple-helix and the telopeptides involving the cross linking sites (87, 930, N-telo and C-telo peptides). A portion of overmodified collagen is transported from the rER into the Golgi, and afterwards into the extracellular space, while a portion of it accumulates in the rER, inducing ER-stress. The secretion of overmodified collagen molecules to the extracellular space leads to abnormal collagen cross-linking in bone, i.e. an increase of HP and a decrease of pyrrole cross-links (hydroxylysyl pyridinoline (HP) , lysyl pyridinoline (LP) , pyrrole ). Both induction of ER-stress and altered collagen cross-linking may contribute to the pathomechanism of OI.

Table 1. Cross-link analysis of dog bone. The mature trivalent cross-links LP and HP from dog bone were quantified by HPLC. In the OI-dog the HP content is increased while the LP content is not altered when compared to controls. Accordingly, the total pyridinoline content (HP+LP) as well as the HP/LP ratio are increased.

Dog Bone		residue/collagen			
Sample type	Mutation	HP	LP	HP+LP	HP/LP
control 14yr		0.11	0.03	0.14	3.7
control 9yr		0.13	0.05	0.18	2.6
OI-dog 10wk	SERPINH1 p.Leu326Pro	0.36	0.05	0.41	7.2

Table 2. Summary and comparison of biochemical data on HSP47 defects in mouse, human and dog. (nd = not determined)

Consequences of HSP47 defect	Mouse ko (18,23)	Human (L78P) (17)	Dog (L326P)
phenotype	embryonic lethal	OI	OI (15)
HSP47 protein instability	(not expressed)	yes	no
Col I overmodification	nd	no	yes
delayed Col I secretion	yes	yes	yes
inefficient Col I processing	yes	nd	yes
abnormal 3-hydroxylation of P986	nd	no	no
accumulation of Col I in	ER	Golgi	ER
ER dilation	yes	nd	yes
Bone cross-linking alterations	nd	nd	yes

Figure 1

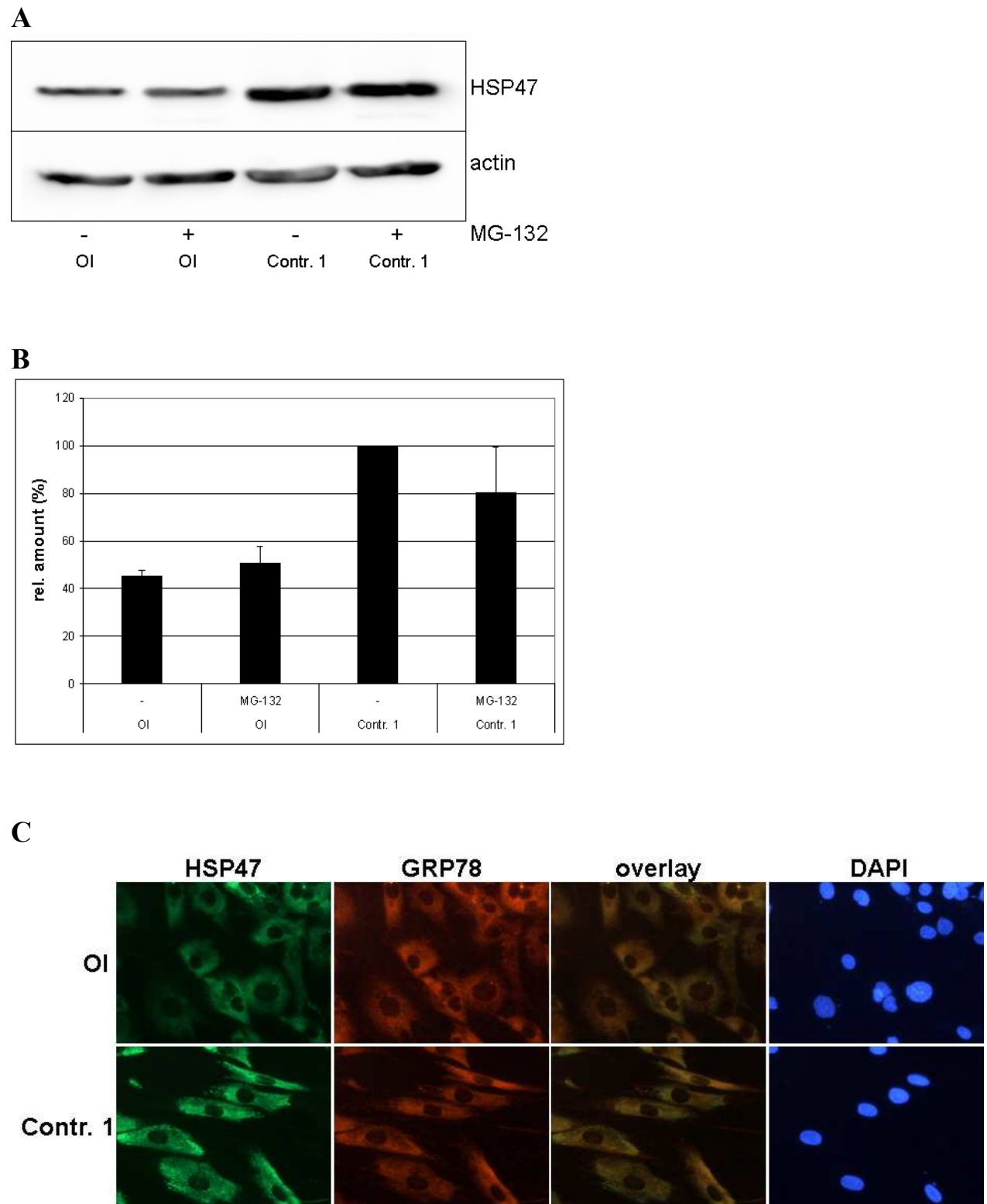
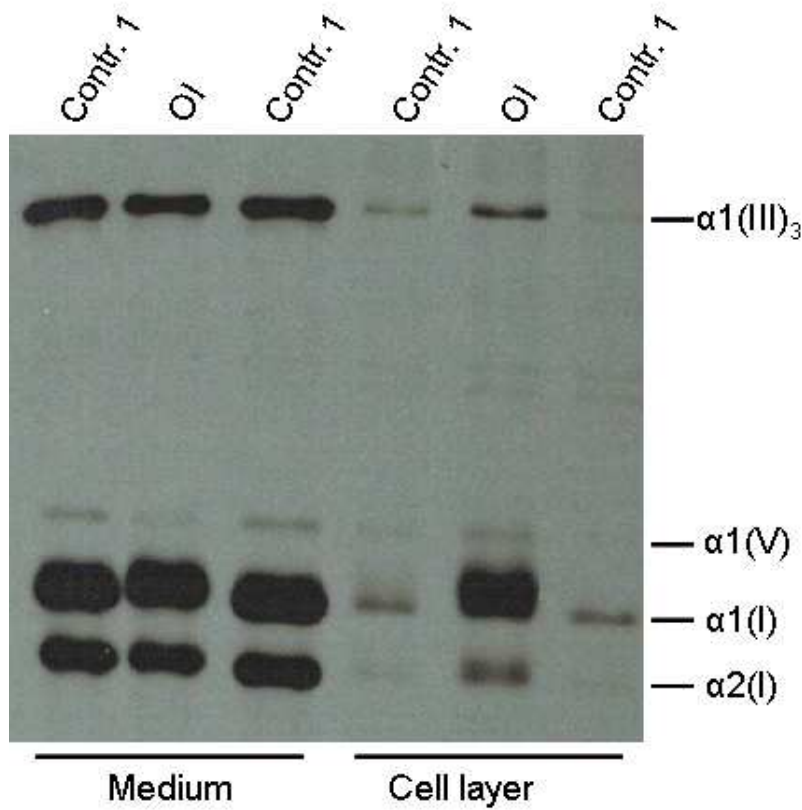


Figure 2

A



B

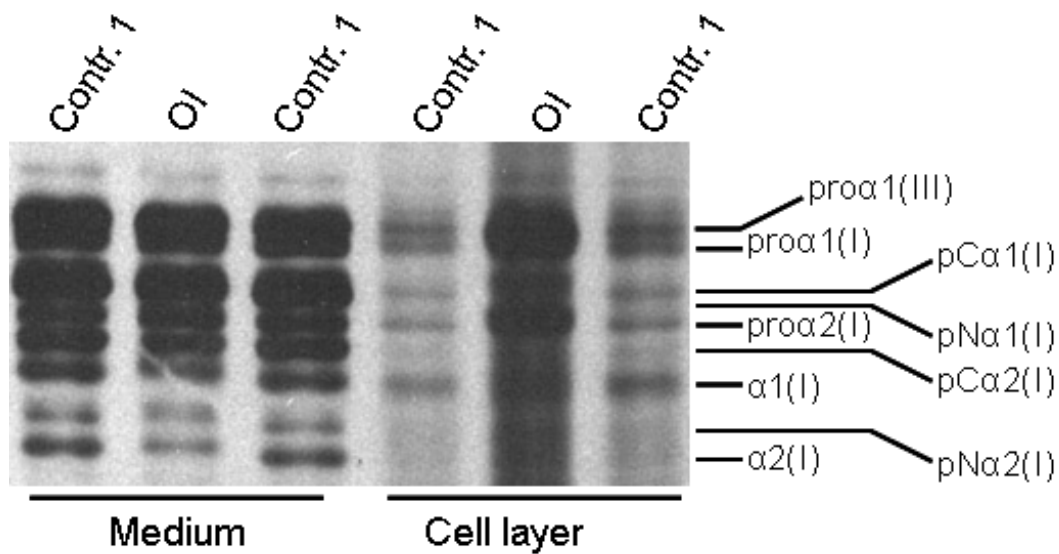


Figure 3

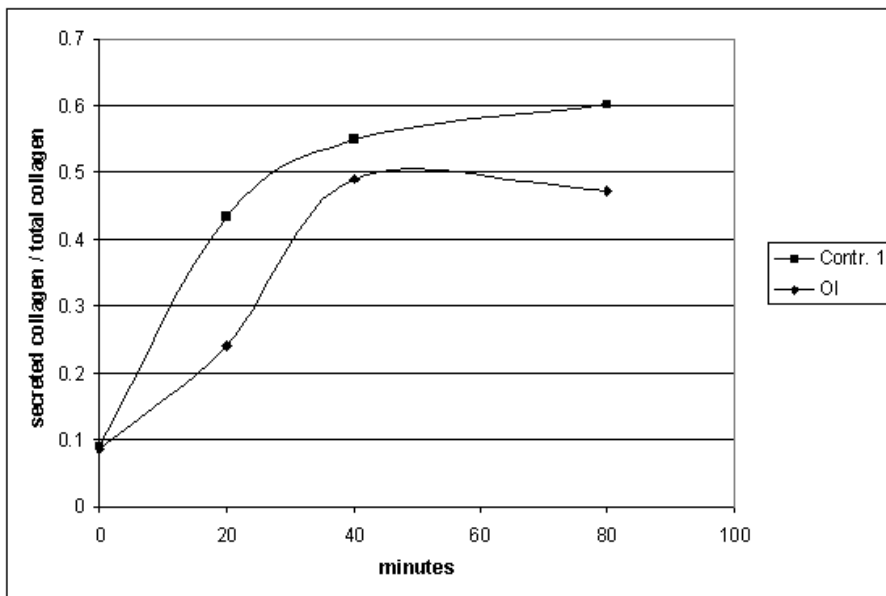
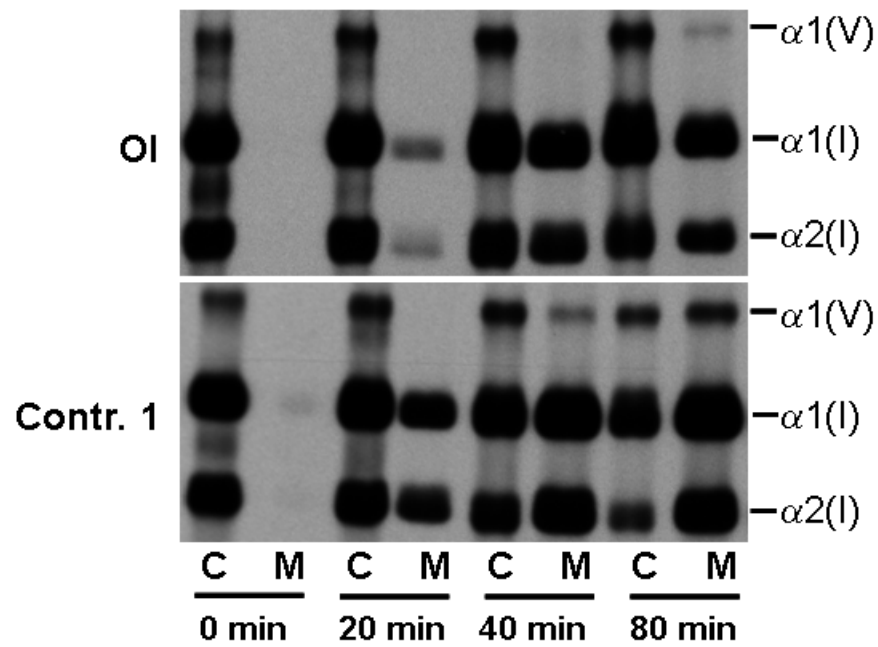
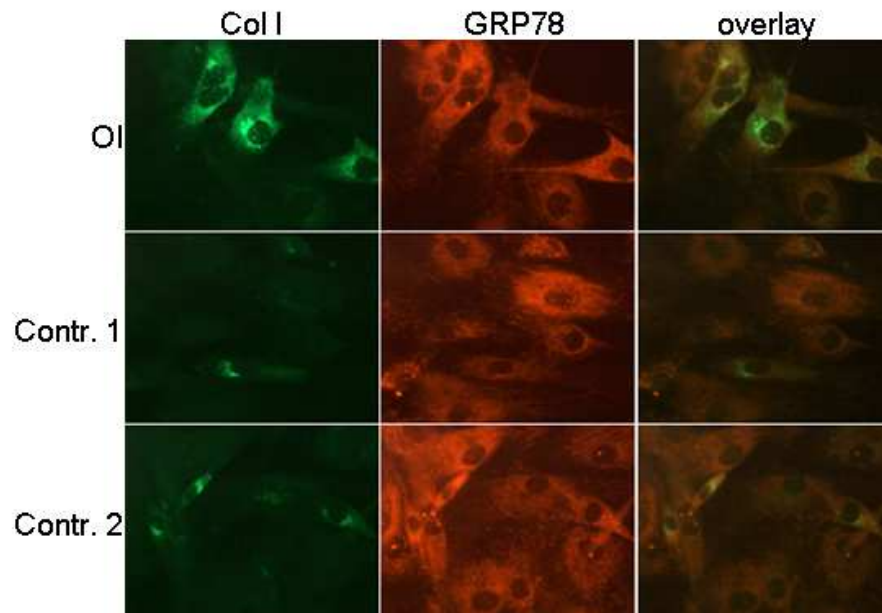


Figure 4

A



B

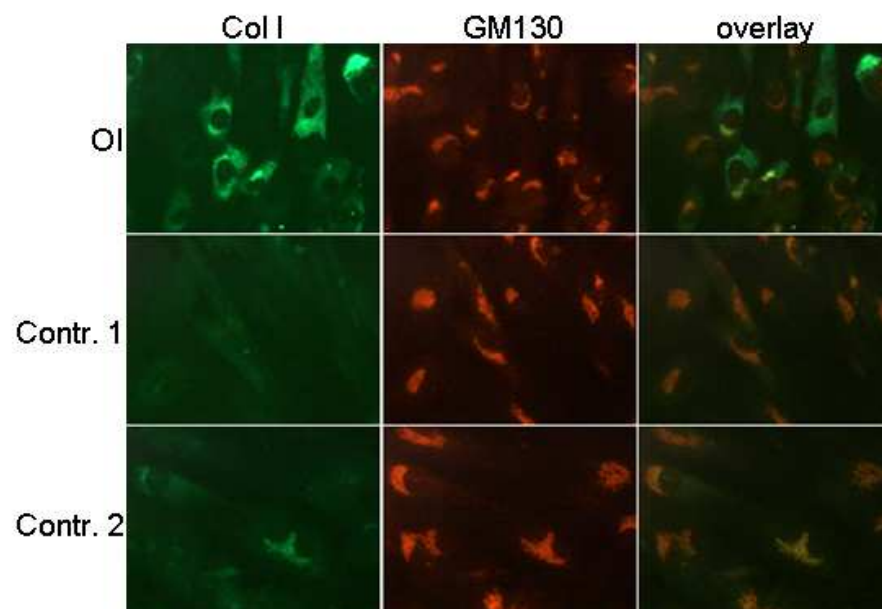


Figure 5

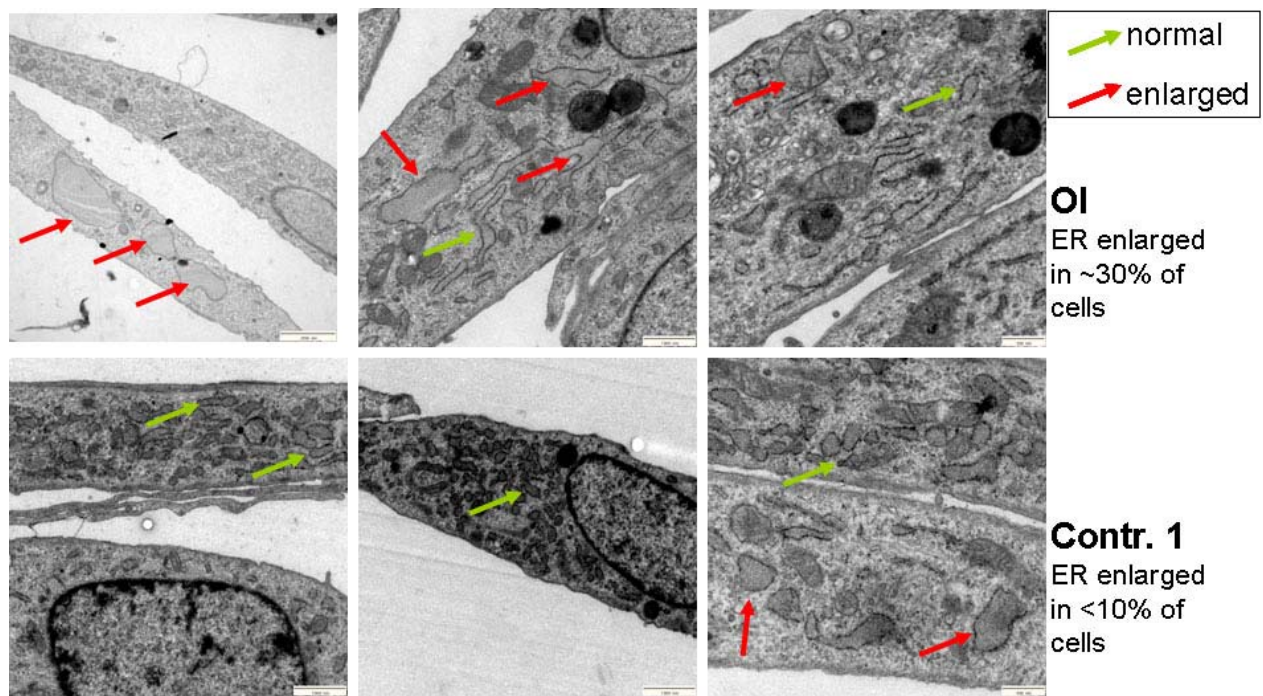


Figure 6

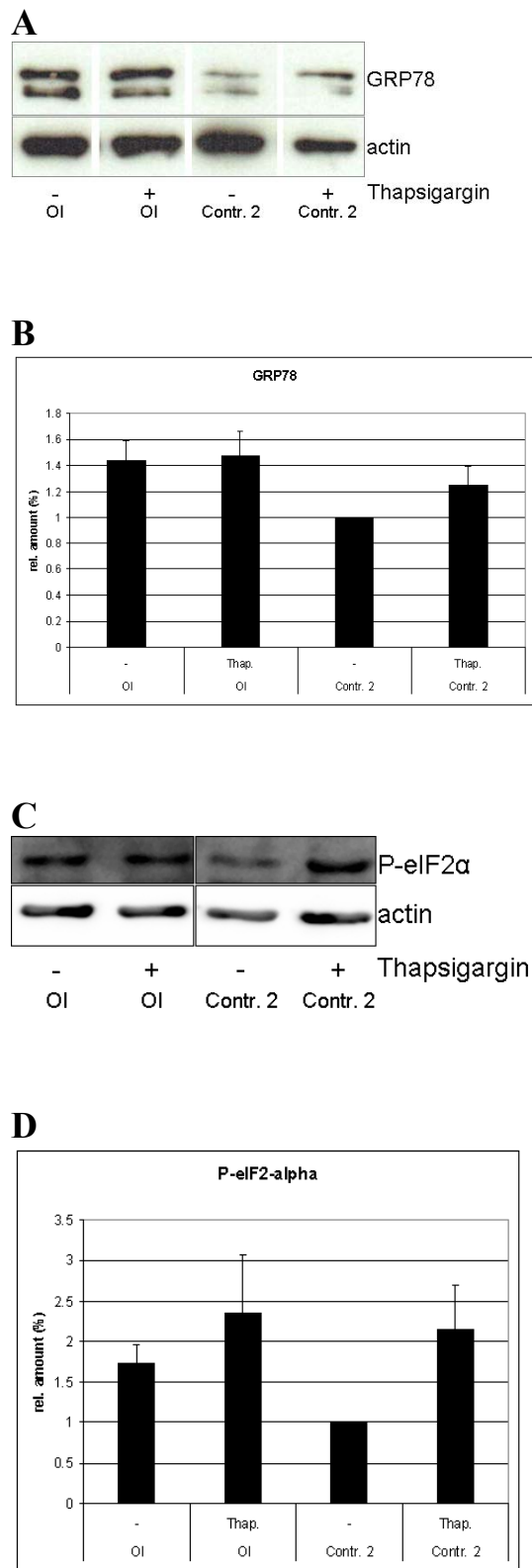


Figure 7

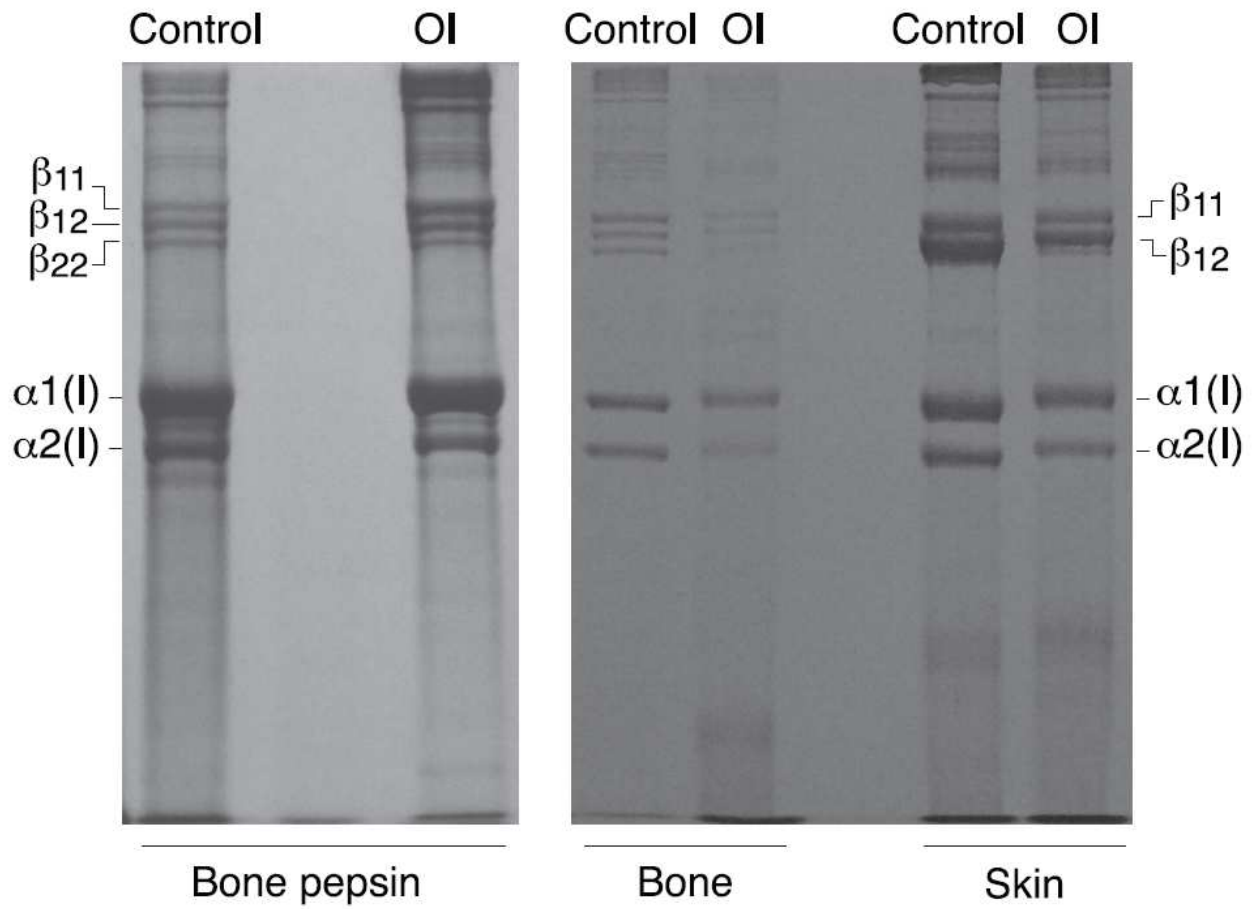


Figure 8

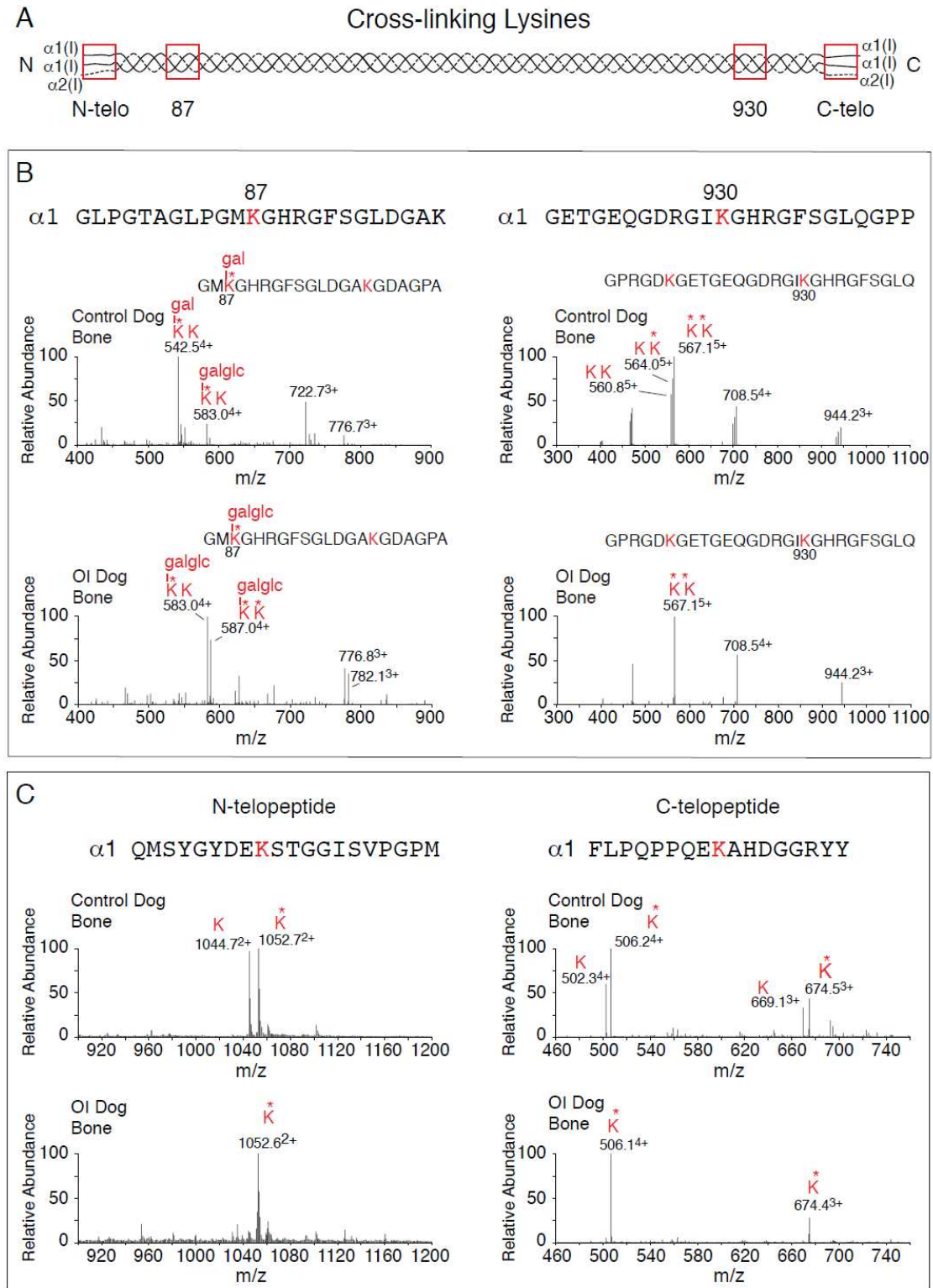
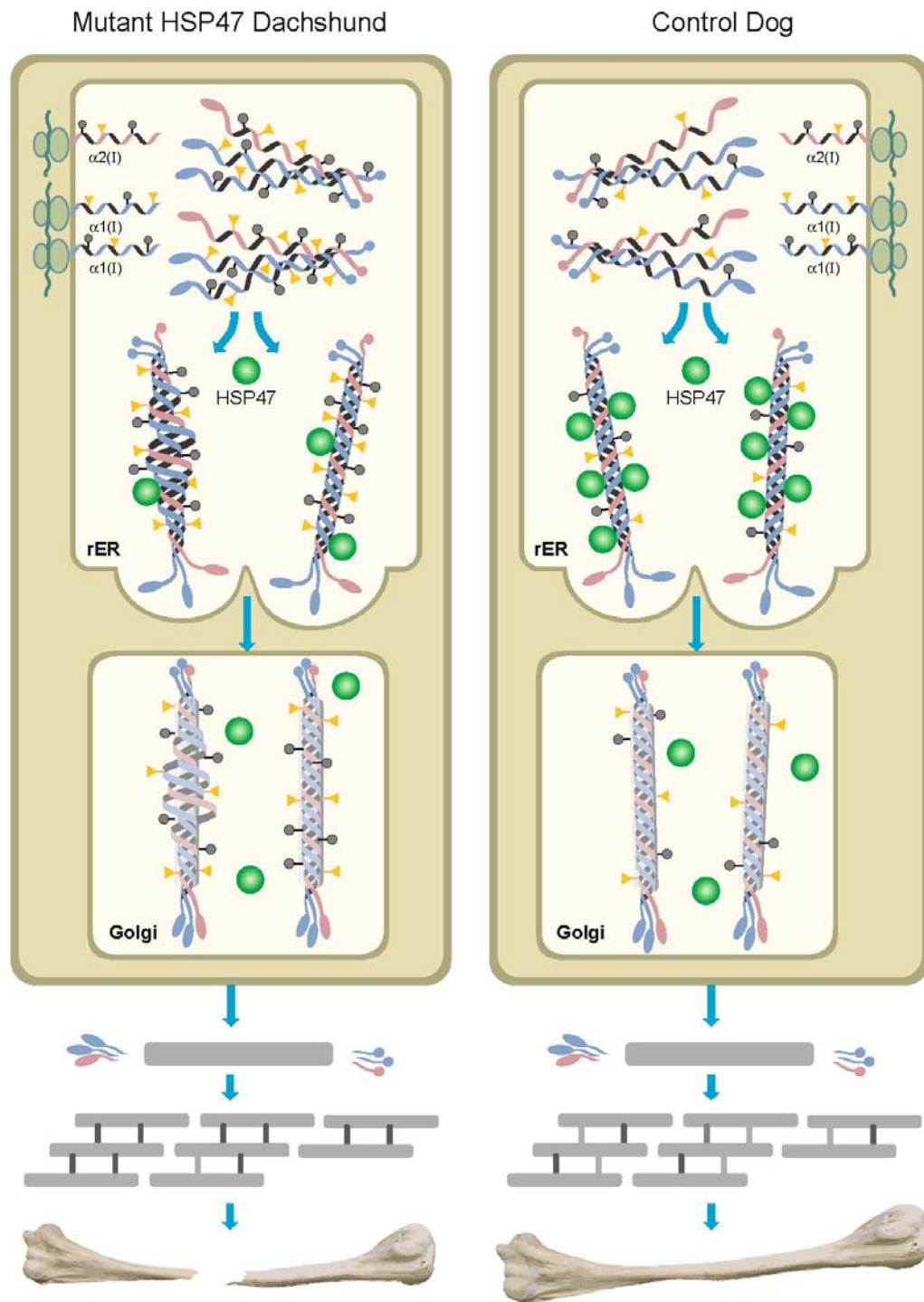


Figure 9



Molecular Consequences of Defective SERPINH1/HSP47 in the Dachshund Natural Model of Osteogenesis Imperfecta

Uschi Lindert, Mary Ann Weis, Jyoti Rai, Frank Seeliger, Ingrid Hausser, Tosso Leeb, David Eyre, Marianne Rohrbach and Cecilia Giunta

J. Biol. Chem. published online May 24, 2015

Access the most updated version of this article at doi: [10.1074/jbc.M115.661025](https://doi.org/10.1074/jbc.M115.661025)

Alerts:

- [When this article is cited](#)
- [When a correction for this article is posted](#)

[Click here](#) to choose from all of JBC's e-mail alerts

This article cites 0 references, 0 of which can be accessed free at
<http://www.jbc.org/content/early/2015/05/24/jbc.M115.661025.full.html#ref-list-1>